# Transport properties of a binary mixture of $CO_2$–$N_2$ from the pair potential energy functions based on a semi-empirical inversion method*

Song Bo(宋 渤), Wang Xiao-Po(王晓坡)†, Yang Fu-Xin(杨富鑫), and Liu Zhi-Gang(刘志刚)

*Key Laboratory of Thermo-Fluid Science and Engineering, Ministry of Education, Xi'an Jiaotong University, Xi'an* 710049*, China*

(Received 7 July 2011; revised manuscript received 26 July 2011)

The potential energy surface of a $CO_2$–$N_2$ mixture is determined by using an inversion method, together with a new collision integral correlation [*J. Phys. Chem. Ref. Data* **19** 1179 (1990)]. With the new invert potential, the transport properties of $CO_2$–$N_2$ mixture are presented in a temperature range from 273.15 K to 3273.15 K at low density by employing the Chapman–Enskog scheme and the Wang Chang–Uhlenbeck–de Boer theory, consisting of a viscosity coefficient, a thermal conductivity coefficient, a binary diffusion coefficient, and a thermal diffusion factor. The accuracy of the predicted results is estimated to be 2% for viscosity, 5% for thermal conductivity, and 10% for binary diffusion coefficient.

**Keywords:** inversion method, potential energy surface, $CO_2$–$N_2$ mixture, transport property

**PACS:** 51.10.+y, 52.25.Fi, 31.50.–x, 34.20.–b **DOI:** 10.1088/1674-1056/21/4/045101

## 1. Introduction

From a statistical mechanics point of view, the macroscopic properties of fluids can be determined by the interactions between molecules. Predictions of transport properties will be straightforward if the potential energy function is already known. Basically, the potential energy function can be obtained through three major ways: theoretical calculations, experimental measurements, and methods combining both of the approaches mentioned above.[1,2] Without using any experimental result, the interaction potential can be accurately calculated from quantum mechanics and some basic assumptions. However, extensive quantum-mechanical calculations have restricted the applications in the case of large atoms with more electrons.[3−8]

On the other hand, due to the fact that there exist quantitative relationships between the information about intermolecular potentials and experimental data, the former can be extracted from the latter. The traditional approach is based on a cut-and-try procedure.[9] Potential parameters, like the well depth $\varepsilon/k$, are varied until the smallest discrepancy is achieved between the calculated and experimental data. In this way, the optimum parameters from one property, say viscosity, may fail to produce another property, say diffusion coefficient. The limitations of the traditional method stimulated the search for more explicit methods. Among them, an inversion scheme was developed in the 1970s[10] by which the interaction potential can be determined directly from transport coefficient data without making any assumption of it. Following the introduction of new equations of reduced collision integrals,[11−13] the inversion scheme has been used as a valuable supplement to quantum-mechanical calculations in determining the potential for a wide variety of substances.[14−18]

The binary mixture of $CO_2$–$N_2$ is a very important substance in many industrial processes, but the thermophysical properties for $CO_2$–$N_2$ mixture must be known previously. For example, the thermophysical properties are needed in the design and the operation of facilities for carbon capture and storage.[19−23] In addition, the $CO_2$–$N_2$ mixture has been considered as a good blowing agent to optimize the structure of polymer foams.[24] Hence, there are great demands for the thermophysical properties of $CO_2$–$N_2$ mixture under different temperature conditions. The thermodynamic properties for $CO_2$–$N_2$ mixture have been studied in the literature.[19,20] To predict their transport properties, the potential energy surface of

*Project supported by the National Natural Science Foundation of China (Grant No. 51006083), the China Postdoctoral Science Foundation (Grant No. 20110491658), and the Fundamental Research Funds for the Central Universities.

†Corresponding author. E-mail: wangxp@mail.xjtu.edu.cn

© 2012 Chinese Physical Society and IOP Publishing Ltd

$CO_2$–$N_2$ mixture is determined in the present work by the inversion method from the principle of corresponding states involving formulas of reduced collision integrals. Based on the new invert potential, dilute viscosity coefficient $\eta_{\rm mix}$, binary diffusion coefficient $D_{12}$, and thermal diffusion factor $\alpha_{\rm T}$ are calculated by the Chapman–Enskog version of kinetic theory. Owing to the influence of the internal degrees of freedom on polyatomic gas, the Wang Chang–Uhlenbeck–de Boer theory[25] is employed to predict the thermal conductivity coefficient $\lambda_{\rm mix}$ at low density. The transport properties of $CO_2$–$N_2$ mixture are reported for a temperature range of 273.15 K to 3273.15 K.

## 2. Theory

### 2.1. Transport properties

The Chapman–Enskog solutions of the Boltzmann equation give the expressions of transport properties for binary mixtures at low density. The formulas of viscosity coefficient $\eta_{\rm mix}$, thermal conductivity coefficient $\lambda_{\rm mix}$, binary diffusion coefficient $D_{12}$, and thermal diffusion factor $\alpha_{\rm T}$ are expressed as follows:[11]

$$\eta_{\rm mix} = \frac{1+Z_\eta}{X_\eta + Y_\eta}, \tag{1}$$

$$\lambda_{\rm mix} = \frac{1+Z_\lambda}{X_\lambda + Y_\lambda}, \tag{2}$$

$$D_{12} = \frac{3}{8}\left[\frac{\pi k^3 T^3 (m_1+m_2)}{2m_1 m_2}\right]^{1/2} \frac{1+\Delta}{P\Omega_{12}^{(1,1)}(T_{12})}, \tag{3}$$

$$\alpha_{\rm T} = (6C_{12}^* - 5)\left(\frac{x_1 S_1 - x_2 S_2}{x_1^2 Q_1 + x_1 x_2 Q_{12} + x_2^2 Q_2}\right) \times (1+\kappa_2), \tag{4}$$

where $k$ is the Boltzmann constant ($1.380658 \times 10^{-23}$ J·K$^{-1}$), $m$ the molecular mass, $x$ the mole fraction, $T$ the temperature, and $P$ the pressure of one atmosphere (101.3 kPa). The correction term $\kappa_2$ in Eq. (4) for $\alpha_{\rm T}$ is small in magnitude and can be neglected in the present calculations. The expressions of the second order correction factor $\Delta$ for $D_{12}$ as well as $S$ and $Q$ listed in Ref. [11] are given as

$$\Delta = 1.3(6C_{12}^* - 5)^2 a x_1/(1+bx_1), \tag{5}$$

$$a = \frac{2^{1/2}}{8(1+1.8c)^2}\frac{\Omega_{12}^{(1,1)}}{\Omega_{22}^{(2,2)}}, \tag{6}$$

$$b = 10a(1+1.8c+3c^2) - 1, \tag{7}$$

$$c = m_2/m_1, \tag{8}$$

$$S_1 = \frac{m_1}{m_2}\left(\frac{2m_2}{m_1+m_2}\right)^{1/2}\frac{\Omega_{11}^{(2,2)}}{\Omega_{12}^{(1,1)}}\left(\frac{\sigma_{11}}{\sigma_{12}}\right)^2 - \frac{4m_1 m_2 A_{12}^*}{(m_1+m_2)^2} + \frac{15m_2(m_1-m_2)}{2(m_1+m_2)^2}, \tag{9}$$

$$Q_1 = \frac{2}{m_2(m_1+m_2)}\left(\frac{2m_2}{m_1+m_2}\right)^{1/2}\frac{\Omega_{11}^{(2,2)}}{\Omega_{12}^{(1,1)}} \times \left(\frac{\sigma_{11}}{\sigma_{12}}\right)^2\left[\left(\frac{5}{2} - \frac{6}{5}B_{12}^*\right)m_1^2 + 3m_2^2 + \frac{8}{5}m_1 m_2 A_{12}^*\right], \tag{10}$$

$$Q_{12} = 15\left(\frac{m_1-m_2}{m_1+m_2}\right)^2\left(\frac{5}{2} - \frac{6}{5}B_{12}^*\right) + \frac{4m_1 m_2 A_{12}^*}{(m_1+m_2)^2}\left(11 - \frac{12}{5}B_{12}^*\right) + \frac{8(m_1+m_2)}{5(m_1 m_2)^{1/2}} \times \left[\frac{\sigma_{11}^2\Omega_{11}^{(2,2)}}{\sigma_{12}^2\Omega_{12}^{(1,1)}}\right]\left[\frac{\sigma_{22}^2\Omega_{22}^{(2,2)}}{\sigma_{12}^2\Omega_{12}^{(1,1)}}\right]. \tag{11}$$

The definitions for $S_2$ and $Q_2$ can be gained from those of $S_1$ and $Q_1$ by exchange of subscripts.

In Eqs. (1) and (2), the quantities $X_\eta$, $Y_\eta$, $Z_\eta$, $X_\lambda$, $Y_\lambda$, and $Z_\lambda$ can be evaluated by[11]

$$X_\eta = \frac{x_1^2}{\eta_1} + \frac{2x_1x_2}{\eta_{12}} + \frac{x_2^2}{\eta_2}, \tag{12}$$

$$Y_\eta = \frac{3}{5}A_{12}^*\left[\frac{x_1^2}{\eta_1}\left(\frac{m_1}{m_2}\right) + \frac{2x_1x_2}{\eta_{12}}\frac{(m_1+m_2)^2}{4m_1m_2} \times \left(\frac{\eta_{12}^2}{\eta_1\eta_2}\right) + \frac{x_2^2}{\eta_2}\left(\frac{m_2}{m_1}\right)\right], \tag{13}$$

$$Z_\eta = \frac{3}{5}A_{12}^*\left\{x_1^2\left(\frac{m_1}{m_2}\right) + 2x_1x_2\left[\frac{(m_1+m_2)^2}{4m_1m_2} \times \left(\frac{\eta_{12}}{\eta_1} + \frac{\eta_{12}}{\eta_2}\right) - 1\right] + x_2^2\left(\frac{m_2}{m_1}\right)\right\}, \tag{14}$$

$$X_\lambda = \frac{x_1^2}{\lambda_1} + \frac{2x_1x_2}{\lambda_{12}} + \frac{x_2^2}{\lambda_2}, \tag{15}$$

$$Y_\lambda = \frac{x_1^2}{\lambda_1}U_1 + \frac{2x_1x_2}{\lambda_{12}}U_Y + \frac{x_2^2}{\lambda_2}U_2, \tag{16}$$

$$Z_\lambda = x_1^2U_1 + 2x_1x_2U_Z + x_2^2U_2. \tag{17}$$

In order to include the contributions of internal degrees of freedom, the expression of thermal conductivity has been modified for polyatomic gas and given in two parts,[25,26]

$$\lambda_{\rm mix_WCUB} = \lambda_{\rm mix} + \sum_{i=1}^{2}(\lambda_{i_\rm WCUB} - \lambda_i) \times \left(1 + \sum_{j=1, j\neq i}^{2} x_j D_{ii}/x_i D_{ij}\right)^{-1}, \tag{18}$$

in which $\lambda_{\rm mix}$ denotes the result calculated directly from Eq. (2) for binary mixture. The second part corresponds to the contributions from translational, rotational, vibrational, and electronic degrees of freedom.

The correlation of $\lambda_{i_\mathrm{WCUB}}$ for pure components can be obtained by

$$\lambda_{i_\mathrm{WCUB}} = \lambda_i + \frac{\eta_i}{m_i}\left(C_{Vi} - \frac{3}{2}R\right) \tag{19}$$

for temperature $T < 350$ K, and

$$\lambda_{i_\mathrm{WCUB}} = \lambda_i + \frac{6\Omega_{ii}^{(2,2)}}{5\Omega_{ii}^{(1,1)}}\frac{\eta_i}{m_i}\left(C_{Vi} - \frac{3}{2}R\right) \tag{20}$$

for temperature $T \geq 350$ K, where $C_{Vi}$ is the molar heat capacity for constant volume, and $R$ the universal gas constant (8.31451 J·mol$^{-1}$·K$^{-1}$).

The dimensionless ratios of collision integrals, which characterize the interactions between all pairs, can be defined as[11]

$$A^* = \Omega^{(2,2)}/\Omega^{(1,1)}, \tag{21}$$
$$B^* = [5\Omega^{(1,2)} - 4\Omega^{(1,3)}]/\Omega^{(1,1)}, \tag{22}$$
$$C^* = \Omega^{(1,2)}/\Omega^{(1,1)}, \tag{23}$$
$$E^* = \Omega^{(2,3)}/\Omega^{(2,2)}, \tag{24}$$
$$F^* = \Omega^{(3,3)}/\Omega^{(1,1)}. \tag{25}$$

## 2.2. Inversion method

According to the kinetic theory of gas, the collision integral $\Omega^{(l,s)}$, giving the information about transport properties, is defined as a function of temperature $T$,[2]

$$\Omega^{(l,s)}(T) = \left[(s+1)!\,(kT)^{s+2}\right]^{-1} \times \int_0^\infty Q^{(l)}(E)\,\mathrm{e}^{-E/kT}E^{s+1}\mathrm{d}E, \tag{26}$$

where $E$ denotes the relative kinetic energy and the numbers $l$ and $s$ are relative to high-order approximation for transport property. The energy-dependent cross section $Q^{(l)}$ has the form,

$$Q^{(l)}(E) = 2\pi\left[1 - \frac{1+(-1)^l}{2(1+l)}\right]^{-1} \times \int_0^\infty \left(1 - \cos^l\theta\right) b\mathrm{d}b, \tag{27}$$

in which $b$ is the impact factor and the scattering angle $\theta$ depends on the collisions between molecules,

$$\theta(E,b) = \pi - 2b\int_{r_0}^\infty \frac{\mathrm{d}r/r^2}{\sqrt{1 - b^2/r^2 - V(r)/E}}, \tag{28}$$

where $r$ is the separation between molecules, $V(r)$ the potential energy surface, and $r_0$ the shortest distance between molecules, which can be solved from the following equation:

$$1 - b^2/r_0^2 - V(r_0)/E = 0. \tag{29}$$

For the inversion scheme, information about potential models and their parameters are not needed. Instead, an arbitrary model, like Lennard–Jones 12-6, can be used as an initial approximation to evaluate the intermolecular potential $V(r)$ by[2]

$$V^* = V(r)/(\varepsilon/k) = G(T^*)\,T^*, \tag{30}$$
$$r^* = r/\sigma = \left(\Omega^{*(2,2)}(T^*)\right)^{1/2}, \tag{31}$$

in which $\varepsilon/k$ is the well depth, $\sigma$ the hard sphere diameter, and $G(T^*)$ the inversion parameters. The superscript * indicates that collision integrals are scaled by $\sigma$, and

$$\Omega^{*(l,s)} = \Omega^{(l,s)}/\pi\sigma^2. \tag{32}$$

$T^*$ denotes the reduced temperature: $T^* = T/(\varepsilon/k)$. The term $\Omega^{*(2,2)}$ as a function of $T^*$ is available from recent extensive sets of corresponding-states correlations.[11–13] The inversion process is repeated by using Eqs. (26)–(32) until convergence. After two or three iterations, the results are very close to true values and the final intermolecular potential can be determined. A brief description of the inversion technique as a flow chart is given in Fig. 1.

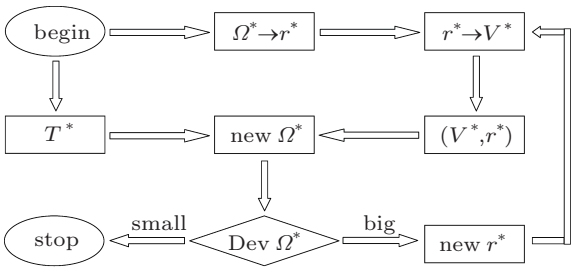



**Fig. 1.** Flow chart of the inversion scheme.

# 3. Results and discussion

Based on the correlation of the reduced collision integral $\Omega^{*(2,2)}(T^*)$,[13] the iterative inversion procedure was employed to generate the interaction potential energy of $CO_2$–$N_2$ gas mixture from the law of corresponding states. The well depth $\varepsilon/k$ and the hard sphere diameter $\sigma$ of $CO_2$–$N_2$, which are needed in the determination of $V(r)$, are 155.0 K and 0.3711 nm respectively.[13] The invert intermolecular potential was used to obtain the ratio of collision integrals for the binary mixture of $CO_2$–$N_2$ from Eqs. (21)–(25). The calculated values of the reduced collision integrals $\Omega^{*(1,1)}$ and $\Omega^{*(2,2)}$ as well as their ratios $A^*$–$F^*$ are displayed in Table 1.

**Table 1.** Reduced collision integrals and their ratios of the binary mixture of $CO_2$–$N_2$ each as a function of reduced temperature.

| $\log T^*$ | $\Omega^{*(1,1)}$ | $\Omega^{*(2,2)}$ | $A^*$ | $B^*$ | $C^*$ | $E^*$ | $F^*$ |
|---|---|---|---|---|---|---|---|
| 0.0 | 1.3788 | 1.5303 | 1.1099 | 1.1897 | 0.8558 | 0.8875 | 0.9268 |
| 0.1 | 1.2523 | 1.3837 | 1.1049 | 1.1629 | 0.8660 | 0.8944 | 0.9339 |
| 0.2 | 1.1465 | 1.2612 | 1.1001 | 1.1395 | 0.8788 | 0.9048 | 0.9431 |
| 0.3 | 1.0594 | 1.1617 | 1.0965 | 1.1213 | 0.8925 | 0.9168 | 0.9536 |
| 0.4 | 0.9882 | 1.0820 | 1.0949 | 1.1086 | 0.9056 | 0.9287 | 0.9642 |
| 0.5 | 0.9295 | 1.0183 | 1.0955 | 1.1012 | 0.9169 | 0.9393 | 0.9740 |
| 0.6 | 0.8805 | 0.9670 | 1.0983 | 1.0982 | 0.9259 | 0.9482 | 0.9827 |
| 0.7 | 0.8385 | 0.9249 | 1.1030 | 1.0986 | 0.9324 | 0.9548 | 0.9900 |
| 0.8 | 0.8015 | 0.8891 | 1.1092 | 1.1009 | 0.9366 | 0.9590 | 0.9964 |
| 0.9 | 0.7678 | 0.8570 | 1.1162 | 1.1038 | 0.9389 | 0.9610 | 1.0021 |
| 1.0 | 0.7364 | 0.8270 | 1.1230 | 1.1063 | 0.9400 | 0.9613 | 1.0071 |
| 1.1 | 0.7067 | 0.7978 | 1.1289 | 1.1079 | 0.9404 | 0.9605 | 1.0115 |
| 1.2 | 0.6782 | 0.7688 | 1.1337 | 1.1087 | 0.9404 | 0.9592 | 1.0151 |
| 1.3 | 0.6508 | 0.7400 | 1.1371 | 1.1088 | 0.9404 | 0.9579 | 1.0178 |
| 1.4 | 0.6246 | 0.7116 | 1.1393 | 1.1083 | 0.9404 | 0.9570 | 1.0198 |
| 1.5 | 0.5994 | 0.6837 | 1.1407 | 1.1075 | 0.9405 | 0.9563 | 1.0211 |
| 1.6 | 0.5753 | 0.6567 | 1.1414 | 1.1067 | 0.9408 | 0.9561 | 1.0219 |
| 1.7 | 0.5523 | 0.6306 | 1.1418 | 1.1058 | 0.9411 | 0.9561 | 1.0225 |
| 1.8 | 0.5304 | 0.6056 | 1.1420 | 1.1049 | 0.9415 | 0.9562 | 1.0230 |
| 1.9 | 0.5094 | 0.5818 | 1.1420 | 1.1042 | 0.9419 | 0.9564 | 1.0234 |
| 2.0 | 0.4895 | 0.5589 | 1.1420 | 1.1036 | 0.9423 | 0.9567 | 1.0239 |

From the invert potential energy surface, the transport properties of the binary mixture of $CO_2$–$N_2$ were calculated at low density. The viscosity coefficient $\eta_{\rm mix}$, the binary diffusion coefficient $D_{12}$, and the thermal diffusion factor $\alpha_{\rm T}$ are obtained by using Eqs. (1), (3), and (4), in a temperature range from 273.15 K to 3273.15 K. For the thermal conductivity coefficient $\lambda_{\rm mix}$, it can be evaluated by employing Eq. (18) to correct its dependence on internal degrees of freedom for polyatomic gas.

As a check of the quality of present work, the comparison between the experimental results about transport properties and the theoretically calculated results is made over a wide temperature range, which are shown in the following Figs. 2–4.

## 3.1. Viscosity

The viscosity data of $CO_2$–$N_2$ mixture were measured at low density by Kestin's group.[27−29] Their measurements were performed with the aid of an oscillating disk instrument, which are very reliable in the considered temperature range. The data given by Kestin and Leidenfrost[27] are in agreement with the theoretically calculated values within ±1.07% at 293.15 K, whereas the best estimate values at 293.15 K and 304.15 K, recommended by Kestin *et al.*,[28] are 0.56% and 0.46% lower than the calculated values. The deviation from the data given by Kestin and Ro[29] is −0.48% at room temperature and it increases up to +1.13% when temperature increases to 873.15 K.

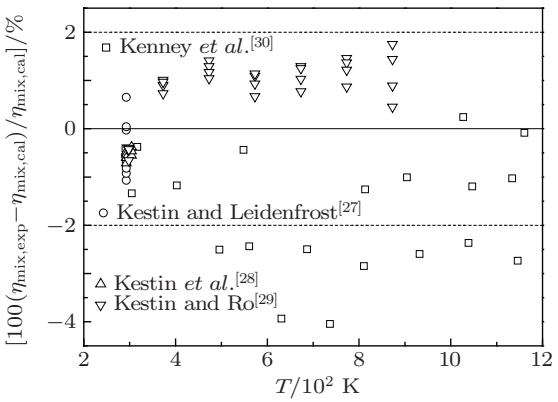



**Fig. 2.** Relative deviations of the experimental viscosity coefficient, $\eta_{\rm mix,exp}$, from the values calculated in the present work, $\eta_{\rm mix,cal}$, for the binary mixture of $CO_2$–$N_2$ at different temperatures.

To validate further the theoretical values at higher temperatures, viscosity data determined by Kenney *et al.*[30] should be considered. They performed relative measurements to determine viscosity values for the mixture of $CO_2$–$N_2$ in a temperature range between 291.35 K and 1160.65 K. The experimental data given

by Kenney *et al.* differ by no more than ±2.85% from the calculated values, with the exception of two data points at 631.15 K and 737.15 K. Figure 2 illustrates that 55 from 64 data points of viscosity measured by Kestin's group and Kenney *et al.* do not deviate by more than ±2% from the theoretical values for the whole temperature range.

## 3.2. Thermal conductivity

In a low pressure gas region, the uncertainty of measurement of thermal conductivity is inferior to that of viscosity due to different experimental problems.[31] As displayed in Fig. 3, all the low-density experimental thermal conductivity data, available in the literature at low, medium, and high temperatures for $CO_2$–$N_2$ mixture,[32−38] are compared with the theoretically calculated values in this work. The experimental values in a temperature range between 273.75 K and 623.15 K were gained from the concentric-cylinder method by Keyes,[32,33] which deviate from the calculated results on average by ±1.69%. Johns *et al.*[34] derived zero-density thermal conductivity data with the transient hot-wire technique in a temperature range from 320 K to 470 K. In principle, the transient hot-wire method is the most accurate technique for determining the thermal conductivity in wide thermodynamic ranges apart from the critical region. The difference between the data given by Johns *et al.* and the theoretical values is −4.27% at 380 K and increases to +1.15% at 470 K with temperature increasing. The data presented by Gilmore and Comings,[35] measured with the concentric-cylinder instruments at 348.15 K, show positive deviations from the calculated values within +4.16%.

At higher temperatures, the data given by Vines[36] and Westenberg and DeHaas[37] were considered for the comparison with the theoretically calculated values. Vines[36] employed the concentric-cylinder apparatus in the laboratory of Keyes to measure thermal conductivity data for $CO_2$–$N_2$ mixture, showing that the obtained data were in accordance with the theoretical values within +2.12% at 1033.15 K. The experimental data sets were gained by Westenberg and DeHaas[37] at high temperatures with line-source method. There occur small deviations ranging from −2.99% to +2.21 % from the data obtained by Westenberg and DeHaas at above 1000 K. It should be stressed that the experimentally measured thermal conductivity data in Refs. [32]–[37] differ from the theoretically calculated values by no more than ±5%.

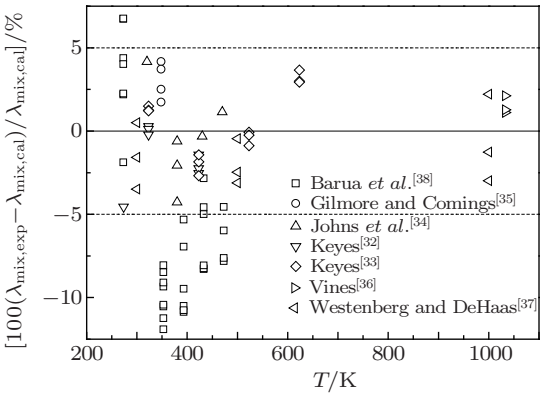



**Fig. 3.** Relative deviations of the experimental thermal conductivity coefficient, $\lambda_{mix,exp}$, from the values calculated in the present work, $\lambda_{mix,cal}$, for the binary mixture of $CO_2$–$N_2$ at different temperatures.

Barua *et al.*[38] reported on one of the most extensive sets of experimental data about thermal conductivity of $CO_2$–$N_2$ mixture. A total of 31 data cover the temperature range from 273.15 K to 473.15 K. The accuracy of all data, however, generally seems to be poor. Figure 3 reveals a large scattering of about ±10% for the data given by Barua *et al.* from the calculated results. The deviations are worst at 353.15 K, while the scatter is smaller at higher temperatures.

## 3.3. Binary diffusion coefficient

There are three sets of experimental binary diffusion coefficient data near ambient temperature reported in the literature.[39−41] Boyd *et al.*[39] carried out measurements by means of a diffusion cell based on the optical method and obtained the results which differ by +4.87% at 293.15 K and +4.83% at 298.15 K from the theoretically calculated values of present paper. The experimental $D_{12}$ value for $CO_2$–$N_2$ mixture at 324.15 K was accurately evaluated by Bohemen and Purnell[40] from chromatographic data. Differences of +2.49% and +1.40 % are found for the data given by Bohemen and Purnell with and without adopting the approximations when solving the van Deemter equation. Robjohns and Dunlop[41] utilized a high-precision Loschmidt-type cell to measure the binary diffusion coefficient in the temperature range from 277 K to 323 K. Robjohns and Dunlop fitted their experimental results to a polynomial as a function of temperature. The polynomial is used to gain binary diffusion data in the steps of 23°, i.e., data at 277 K, 300 K, and 323 K, thereby resulting in a deviation up to +5.83%.

For temperatures above ambient temperature, the experimental data obtained by Ellis and Holsen[42] from the flow measurements through a porous medium, deviate by ±5.55% on average from the theoretical values in a temperature range from 300 K to 900 K. In addition, the experimental data between 290.4 K and 473.0 K obtained by Ivakin and Suetin's[43] utilizing the optical method are characterized by positive differences raging from +5.45% to +9.53%, apart from the data point at 290.4 K. Among the experimentally measured $D_{12}$ data extending to high temperatures, those given by Schneider and Schäfer[44] above 1000 K deviate by ±(6.71–8.58)% from the calculated values, whereas the data measured by Walker and Westenberg's[45] using the point source technique, differ by +10.68% at 1200 K. Figure 4 shows obviously that most of the measurements yielded $D_{12}$ data which accord with the calculated values of the present work within ±10% in the complete temperature range.

There are few accurate experimental data available in the literature and can hardly provide an adequate basis for the comparison of $\alpha_T$, which are not included in this work. The predicted results are given in Tables 2–4 for viscosity $\eta_{mix}$, thermal conductivity $\lambda_{mix}$, binary diffusion coefficient $D_{12}$, and thermal diffusion factor $\alpha_T$. The tables contain the transport properties of $CO_2$–$N_2$ mixture at three different mole fractions in a temperature range between 273.15K and 3273.15 K.

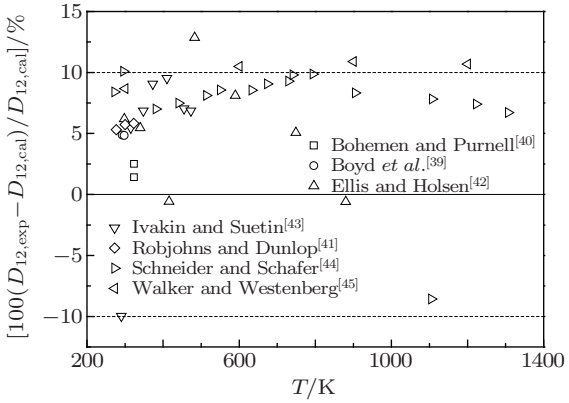



**Fig. 4.** Relative deviations of the experimental binary diffusion coefficient, $D_{12,exp}$, from the values calculated in the present work, $D_{12,cal}$, for the binary mixture of $CO_2$–$N_2$ at different temperatures.

**Table 2.** Transport properties of the binary mixture of $CO_2$–$N_2$ at $x_{CO_2} : x_{N_2} = 0.25 : 0.75$ as a function of temperature.

| $T$/K | $\eta_{mix}$/μPa·s | $\lambda_{mix}$/mW·m$^{-1}$·K$^{-1}$ | $D_{12}$ (101.3 kPa)/$10^{-4}$ m$^2$·s$^{-1}$ | $\alpha_T$ |
|---|---|---|---|---|
| 273.15 | 16.10 | 20.99 | 0.1336 | 0.0740 |
| 293.15 | 17.05 | 22.31 | 0.1521 | 0.0794 |
| 313.15 | 17.98 | 23.62 | 0.1716 | 0.0843 |
| 333.15 | 18.88 | 24.90 | 0.1921 | 0.0888 |
| 353.15 | 19.76 | 28.26 | 0.2134 | 0.0929 |
| 373.15 | 20.61 | 29.64 | 0.2357 | 0.0966 |
| 423.15 | 22.66 | 33.05 | 0.2949 | 0.1044 |
| 473.15 | 24.60 | 36.40 | 0.3592 | 0.1106 |
| 523.15 | 26.45 | 39.71 | 0.4282 | 0.1155 |
| 573.15 | 28.22 | 42.97 | 0.5018 | 0.1194 |
| 623.15 | 29.91 | 46.20 | 0.5799 | 0.1226 |
| 673.15 | 31.55 | 49.40 | 0.6622 | 0.1251 |
| 723.15 | 33.13 | 52.57 | 0.7487 | 0.1271 |
| 773.15 | 34.67 | 55.71 | 0.8392 | 0.1287 |
| 873.15 | 37.61 | 61.89 | 1.0321 | 0.1311 |
| 973.15 | 40.43 | 67.94 | 1.2403 | 0.1327 |
| 1073.15 | 43.13 | 73.83 | 1.4631 | 0.1338 |
| 1173.15 | 45.73 | 79.56 | 1.7003 | 0.1345 |
| 1273.15 | 48.26 | 85.14 | 1.9515 | 0.1349 |
| 1773.15 | 60.00 | 110.8 | 3.4052 | 0.1354 |
| 2273.15 | 70.70 | 133.7 | 5.1672 | 0.1351 |
| 2773.15 | 80.70 | 154.9 | 7.2143 | 0.1348 |
| 3273.15 | 90.15 | 174.6 | 9.5292 | 0.1346 |

**Table 3.** Transport properties of the binary mixture of $CO_2$–$N_2$ at $x_{CO_2} : x_{N_2} = 0.50 : 0.50$ as a function of temperature.

| $T$/K | $\eta_{mix}$/μPa·s | $\lambda_{mix}$/mW·m$^{-1}$·K$^{-1}$ | $D_{12}$ (101.3 kPa)/$10^{-4}$ m$^2$·s$^{-1}$ | $\alpha_T$ |
|---|---|---|---|---|
| 273.15 | 15.36 | 18.61 | 0.1337 | 0.0681 |
| 293.15 | 16.33 | 19.94 | 0.1523 | 0.0732 |
| 313.15 | 17.28 | 21.27 | 0.1719 | 0.0778 |
| 333.15 | 18.20 | 22.59 | 0.1924 | 0.0821 |
| 353.15 | 19.11 | 26.15 | 0.2138 | 0.0860 |
| 373.15 | 19.99 | 27.62 | 0.2361 | 0.0895 |
| 423.15 | 22.11 | 31.26 | 0.2955 | 0.0970 |
| 473.15 | 24.13 | 34.86 | 0.3600 | 0.1030 |
| 523.15 | 26.05 | 38.42 | 0.4294 | 0.1077 |
| 573.15 | 27.89 | 41.93 | 0.5033 | 0.1115 |
| 623.15 | 29.65 | 45.39 | 0.5817 | 0.1146 |
| 673.15 | 31.35 | 48.81 | 0.6644 | 0.1170 |
| 723.15 | 33.00 | 52.18 | 0.7513 | 0.1190 |
| 773.15 | 34.59 | 55.51 | 0.8422 | 0.1206 |
| 873.15 | 37.63 | 62.02 | 1.0360 | 0.1229 |
| 973.15 | 40.52 | 68.33 | 1.2451 | 0.1245 |
| 1073.15 | 43.29 | 74.46 | 1.4689 | 0.1255 |
| 1173.15 | 45.95 | 80.40 | 1.7072 | 0.1262 |
| 1273.15 | 48.53 | 86.15 | 1.9594 | 0.1266 |
| 1773.15 | 60.41 | 112.5 | 3.4193 | 0.1270 |
| 2273.15 | 71.19 | 135.9 | 5.1887 | 0.1267 |
| 2773.15 | 81.24 | 157.6 | 7.2443 | 0.1264 |
| 3273.15 | 90.74 | 177.6 | 9.5688 | 0.1262 |

**Table 4.** Transport properties of the binary mixture of $CO_2$–$N_2$ at $x_{CO_2} : x_{N_2} = 0.75 : 0.25$ as a function of temperature.

| $T$/K | $\eta_{mix}$/μPa·s | $\lambda_{mix}$/mW·m$^{-1}$·K$^{-1}$ | $D_{12}$ (101.3 kPa)/$10^{-4}$ m$^2$·s$^{-1}$ | $\alpha_T$ |
|---|---|---|---|---|
| 273.15 | 14.60 | 16.48 | 0.1338 | 0.0630 |
| 293.15 | 15.57 | 17.82 | 0.1524 | 0.0678 |
| 313.15 | 16.53 | 19.17 | 0.1721 | 0.0722 |
| 333.15 | 17.46 | 20.51 | 0.1926 | 0.0763 |
| 353.15 | 18.38 | 24.21 | 0.2141 | 0.0800 |
| 373.15 | 19.28 | 25.74 | 0.2364 | 0.0834 |
| 423.15 | 21.46 | 29.58 | 0.2961 | 0.0906 |
| 473.15 | 23.53 | 33.38 | 0.3608 | 0.0964 |
| 523.15 | 25.52 | 37.15 | 0.4304 | 0.1010 |
| 573.15 | 27.42 | 40.87 | 0.5046 | 0.1046 |
| 623.15 | 29.25 | 44.54 | 0.5833 | 0.1076 |
| 673.15 | 31.01 | 48.15 | 0.6663 | 0.1100 |
| 723.15 | 32.70 | 51.70 | 0.7535 | 0.1119 |
| 773.15 | 34.34 | 55.19 | 0.8448 | 0.1135 |
| 873.15 | 37.48 | 62.00 | 1.0394 | 0.1158 |
| 973.15 | 40.45 | 68.56 | 1.2493 | 0.1173 |
| 1073.15 | 43.29 | 74.90 | 1.4741 | 0.1183 |
| 1173.15 | 46.00 | 81.02 | 1.7132 | 0.1189 |
| 1273.15 | 48.62 | 86.94 | 1.9664 | 0.1193 |
| 1773.15 | 60.65 | 113.9 | 3.4319 | 0.1198 |
| 2273.15 | 71.49 | 137.8 | 5.2078 | 0.1194 |
| 2773.15 | 81.58 | 159.9 | 7.2711 | 0.1191 |
| 3273.15 | 91.12 | 180.3 | 9.6042 | 0.1189 |

# 4. Conclusion

In the present work, by using a new correlation of the reduced collision integral $\Omega^{*(2,2)}(T^*)$, the pair potential energy function of $CO_2$–$N_2$ mixture is determined based on the inversion procedure from the principle of corresponding states. Furthermore, according to the Chapman–Enskog version of kinetic theory, the transport properties of $CO_2$–$N_2$ mixture are calculated at low density from the new invert potential energy surface, including viscosity coefficient $\eta_{\rm mix}$, binary diffusion coefficient $D_{12}$, and thermal diffusion factor $\alpha_{\rm T}$. To consider the contributions of internal degrees of freedom to polyatomic gas, the Wang Chang–Uhlenbeck–de Boer theory is used to evaluate the thermal conductivity coefficient $\lambda_{\rm mix}$ for the binary mixture of $CO_2$–$N_2$. The predicted results of transport properties are presented for the temperature ranging from 273.15 K to 3273.15 K. The deviations of experimental data from the theoretically calculated values are $\pm 2\%$ for $\eta_{\rm mix}$, $\pm 5\%$ for $\lambda_{\rm mix}$, and $\pm 10\%$ for $D_{12}$. The good agreement between the experimental data and the predicted results shows that the inversion method is a useful tool to determine interaction potentials. The invert potentials are able to produce accurate transport properties for binary mixtures of polyatomic gas, which is a valuable supplement to experimental measurements.

# References


[1] Hirschfelder J O, Curtiss C F and Bird R B 1954 *Molecular Theory of Gases and Liquids* (New York: John Wiley)

[2] Maitland G C, Rigby M, Smith E B and Wakeham W A 1984 *Intermolecular Forces: Their Origin and Determination* (Oxford: Clarendon Press)

[3] Yu J X, Fu M, Ji G F and Chen X R 2009 *Chin. Phys.* B **18** 269

[4] Liu X, Zhou X M and Zeng Z Y 2010 *Chin. Phys.* B **19** 127103

[5] Wang Z Q, Zhang C Z, Yu H J, Du J M and Ma J G 2011 *Chin. Phys.* B **20** 033107

[6] Jiang N and Cao Z X 2010 *Acta Phys. Sin.* **59** 3324 (in Chinese)

[7] Chen G F, Gong M Q, Shen J, Zou X and Wu J F 2010 *Acta Phys. Sin.* **59** 8669 (in Chinese)

[8] Song B, Wang X P, Wu J T and Liu Z G 2011 *Acta Phys. Sin.* **60** 033401 (in Chinese)

[9] Barker J A, Watts R O, Lee J K, Schafer T P and Lee Y T 1974 *J. Chem. Phys.* **61** 3081

[10] Clancy P, Gough D W, Matthews G P, Smith E B and Maitland G C 1975 *Mol. Phys.* **30** 1397

[11] Kestin J, Knierim K, Mason E A, Najafi B, Ro S T and Waldman M 1984 *J. Phys. Chem. Ref. Data* **13** 229

[12] Boushehri A, Bzowski J, Kestin J and Mason E A 1987 *J. Phys. Chem. Ref. Data* **16** 445

[13] Bzowski J, Kestin J, Mason E A and Uribe F J 1990 *J. Phys. Chem. Ref. Data* **19** 1179

[14] Boushehri A and Maghari A 1990 *J. Phys. Soc. Jpn.* **59** 4302

[15] Behnejad H, Maghari A and Najafi M 1995 *J. Comput. Chem.* **16** 441

[16] Najafi M and Haghighi B 2000 *Indian J. Pure Appl. Phys.* **38** 229

[17] Behnejad H, Hosseinnejad T, Shahmir V H and Arianfar F 2005 *Chem. Phys.* **311** 245

[18] Wang X P, Song B, Wu J T and Liu Z G 2010 *Acta Phys. Sin.* **59** 7158 (in Chinese)

[19] Li H and Yan J 2009 *Appl. Energy* **86** 826

[20] Li H and Yan J 2009 *Appl. Energy* **86** 2760

[21] Herri J M, Bouchemoua A, Kwaterski M, Fezoua A, Ouabbas Y and Cameirao A 2011 *Fluid Phase Equilib.* **301** 171

[22] Zhu F, Dong S and Cheng G 2011 *Chin. Phys.* B **20** 077103

[23] E P, Duan P, Wei L Q, Bai D Y, Jiang B H and Xu D G 2010 *Acta Phys. Sin.* **59** 8676 (in Chinese)

[24] Di Maio E, Mensitieri G, Iannace S, Nicolais L, Li W and Flumerfelt R W 2005 *Polym. Eng. Sci.* **45** 432

[25] Wang Chang C S, Uhlenbeck G E and de Boer J 1964 *The Heat Conductivity and Viscosity of Polyatomic Gases* (New York: Wiley)

[26] Uribe F J, Mason E A and Kestin J 1991 *Int. J. Thermophys.* **12** 43

[27] Kestin J and Leidenfrost W 1959 *Physica* **25** 525

[28] Kestin J, Kobayash Y and Wood R T 1966 *Physica* **32** 1065

[29] Kestin J and Ro S T 1974 *Ber. Bunsenges. Phys. Chem.* **78** 20

[30] Kenney M J, Sarjant R J and Thring M W 1956 *Br. J. Appl. Phys.* **7** 324

[31] Assael M J, Antoniadis K D and Wakeham W A 2010 *Int. J. Thermophys.* **31** 1051

[32] Keyes F G 1951 *Trans. ASME* **73** 597

[33] Keyes F G 1952 *Trans. ASME* **74** 1303

[34] Johns A I, Rashid S, Rowan L, Watson J T R and Clifford A A 1988 *Int. J. Thermophys.* **9** 3

[35] Gilmore T F and Comings E W 1966 *AIChE J.* **12** 1172

[36] Vines R 1960 *J. Heat Trans.* **82** 48

[37] Westenberg A A and DeHaas N 1962 *Phys. Fluids* **5** 266

[38] Barua A K, Manna A and Mukhopadhyay P 1968 *J. Phys. Soc. Jpn.* **25** 862

[39] Boyd C A, Stein N, Steingrimsson V and Rumpel W F 1951 *J. Chem. Phys.* **19** 548

[40] Bohemen J and Purnell J H 1961 *J. Chem. Soc.* **36** 360

[41] Robjohns H L and Dunlop P J 1984 *Ber. Bunsenges. Phys. Chem.* **88** 1239

[42] Ellis C S and Holsen J N 1969 *Ind. Eng. Chem. Fundamen.* **8** 787

[43] Ivakin B A and Suetin P E 1964 *Sov. Phys. Tech. Phys.* **9** 866

[44] Schneide M and Schäfer K 1969 *Ber. Bunsenges. Phys. Chem.* **73** 702

[45] Walker R E and Westenberg A A 1958 *J. Chem. Phys.* **29** 1147